Titanium Aluminide: Electron Beam Weldability

Ingots processed with a proprietary technique along with careful parameter control resulted in good weldability

BY R. A. PATTERSON, P. L. MARTIN, B. K. DAMKROGER AND L. CHRISTODOULOU

ABSTRACT. The weldability of Ti-48 at.-% Al-6.5 vol-% TiB_2 alloy was assessed using autogenous electron beam welding. This material was made by the Martin Marietta Research Laboratories' technique called XD®[1] which introduces a particulate reinforcement phase during ingot processing. In this instance, the particulate phase was TiB_2. Weldability of the material was determined to be very good and high quality bead-on-plate welds were produced when process parameters were properly chosen. However, a susceptibility to solid-state cracking was observed when welding conditions resulted in calculated heat-affected zone cooling rates in excess of 300 K/s. Two possible explanations for this cooling rate dependence are suggested: one based upon the development of thermally induced stresses and the other on observed microstructural changes that promote limitations in strain accommodation.

Introduction

Ordered intermetallic alloys based upon aluminides are rapidly emerging as attractive materials for high-temperature structural applications. Advantages of these alloys over conventional nickel-based superalloys or titanium alloys include the following: high specific modulus, high recrystallization temperatures, and low self-diffusion, which leads to improved creep, high-temperature fatigue and high-temperature oxidation resistance (Refs. 1-3). Research aimed at developing fundamental understanding and processing experience for aluminides has matured to the point of evaluating potential applications, mainly in the aerospace industry (Ref. 4). However, the effective utilization of these alloys has been hampered by their limited fabricability, a direct consequence of poor ductility.

Santella, *et al.*, has shown that in the case of Ni_3Al, one manifestation of this poor fabricability is a susceptibility to weld cracking (Ref. 5). The hafnium additions (0.5 at.-%) to Ni_3Al alloy were shown to significantly reduce susceptibility to weld cracking (Ref. 6). Weld cracking has also been observed in a Ti_3Al-Nb alloy (Ref. 7), but the weldability of TiAl has not been investigated.

This investigation evaluated the electron beam weldability of Ti-48 at.-% Al reinforced with 6.5 vol-% TiB_2. This material was produced by Martin Marietta Laboratories using the patented XD process. The particulate reinforcement is directly responsible for grain size refinement that results in improved casting and thermomechanical processing characteristics when compared with unreinforced base alloy (Ref. 8). This suggests that secondary processing such as fusion welding would be enhanced as well.

Materials and Experimental Approach

The XD process was used to produce an induction skull melted ingot of nominal composition Ti-48 at.-% Al with 6.5 vol-% TiB_2 reinforcement, hereafter referred to as XD TiAl. The chemical analysis of this material is given in Table 1. The titanium-aluminum phase diagram of McCullough, *et al.* (Fig. 1), shows that this alloy was a near gamma composition (Ref. 9). The ingot was isothermally forged in the alpha-plus-gamma phase region and air cooled. No additional heat treatment was used. Weld coupons 25 × 75 × 2.5 mm (1 × 3 × 0.1 in.) thick were removed from the forged ingot by electro-discharge maching (EDM). Prior to welding, coupons were ground to remove approximately 0.1 mm (0.004 in.) from each surface to eliminate the EDM-affected layer, degreased and rinsed in ethanol.

The microstructure of the parent metal is shown in Fig. 2 and consists of three major microconstituents. Deformed alpha-2 (DO_{19} crystal structure) and gamma ($L1_0$ crystal structure) lamellar colonies, approximately 50 by 20 μm in size, are believed to be untransformed during the isothermal forging step, and therefore, representative of the as-cast microstructure. Equiaxed grains of alpha-2 and gamma, approximately 20 μm in diameter, are also observed and are apparently a result of dynamic recrystallization or solid-state transformations during cool down from the forging temperature. Blocky TiB_2 particulates are randomly dispersed throughout the matrix and have an average size of approximately 10 μm — Fig. 2. Reported size distributions for the TiB_2 in

KEY WORDS

Titanium Aluminide
Ti-48Al/6.5vol-%TiB_2
Electron Beam Weld
EB Weldability
XD Processing
Crack Susceptibility
Ordered Alloys
Intermetallic Alloys
Solid-State Cracking
Induced Stresses

Table 1—Alloy Composition (excluding TiB_2)

Element	at.-%	wt-%
Ti	Bal.	Bal.
Al	48.0	34.4
O	0.358	0.152
N	0.032	0.012
C	0.017	0.054

R. A. PATTERSON, P. L. MARTIN and B. K. DAMKROGER are with Materials Technology, Metallurgy Group, Los Alamos National Laboratory, Los Alamos, N.Mex. L. CHRISTODOULOU is with Martin Marietta Laboratories, Baltimore, Md.

1. *XD is a registered trademark of Martin Marietta Corp.*

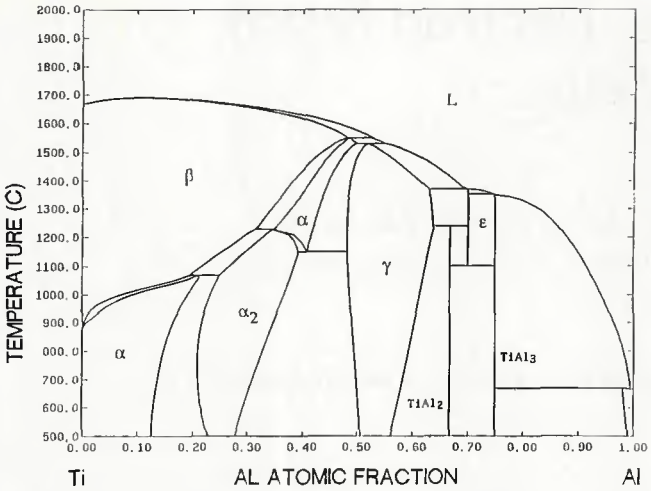

Fig. 1 — Titanium-aluminum binary phase diagram of McCullough, et al. (Ref. 9).

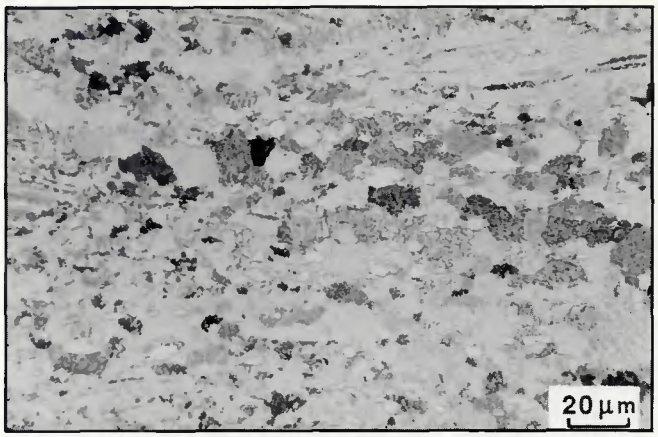

Fig. 2 — Photomicrograph of the XD® Ti-4B at.-% Al-6.5 vol-% TiB_2, base metal. Microstructure consists of lamellar alpha-2-plus-gamma colonies, equiaxed alpha-2 and gamma grains, and blocky TiB_2 particulates. Modified Kroll's etch.

this alloy average 1.8 µm, indicating that a large fraction of the particulates are too fine to be resolved by optical microscopy (Ref. 10).

Welding trials were performed using a 7.5 kW Hamilton Standard electron beam system that had been retrofitted with Leybold Heraeus IKE fast-beam current control and the ribbon filament gun. Additionally, all welds were monitored with a Keithley Soft 500 data-acquisition system and a Leybold Heraeus CCD video monitoring system. A conventional plate fixture using minimal clamping force was used to hold samples during welding and cartridge heaters were added for the application of controlled preheat. Table 2 lists the weld parameters used during this evaluation. Weld travel speed and preheat were the principal variables used to alter thermal profiles, and beam power was adjusted to achieve full penetration. Only full penetration welds were evaluated. The various combinations of welding parameters were normalized using a relative heat-affected zone cooling rate (HAZ CR). Cooling rates were calculated using a Rosenthal two-dimensional heat flow analysis and average thermophysical properties for Ti_3Al-Nb, super alpha-2 alloy (Ref. 11 and 7). All cooling rates were calculated at the fusion boundary and reported as an average cooling rate over the temperature range of 1400° to 800°C (2552° to 1472°F). Equation 1 shows the formulation and associated thermal properties used for this calculation.

$$T - T_0 = ((q/v)/d(4\pi\lambda\rho ct)^{(1/2)})\exp(-r^2/4\alpha t)$$

where:

q = heat input in watts
v = weld speed in m/s
d = plate thickness in m
λ = thermal conductivity, 16.6 J/msK
ρ c = volumetric thermal capacity, 3.25×10^6 J/m^{3}K
t = time (1400° to 800°C) in seconds
α = thermal diffusivity, 9.0×10^{-6} m^2/s
r = radius from weld centerline in m

Weldability was evaluated as the resistance to weld cracking induced by restraint of the specimen. Postweld examination was performed with a Mitutoyo toolmakers microscope at 50X magnification. Microhardness measurements were made using a Shimadzu diamond pyramid hardness (DPH) tester with a 200-g load. Specimens were prepared for metallography using standard techniques and modified Kroll's reagent (5 vol-% HF, 35 vol-% HNO_3) as an etchant. Compositional variations within weld fusion zones were characterized by energy dispersive spectroscopy (EDS) on metallographic cross-sections. Fracture surfaces were examined with scanning electron microscopy (SEM). No surface preparation was used on fractography specimens.

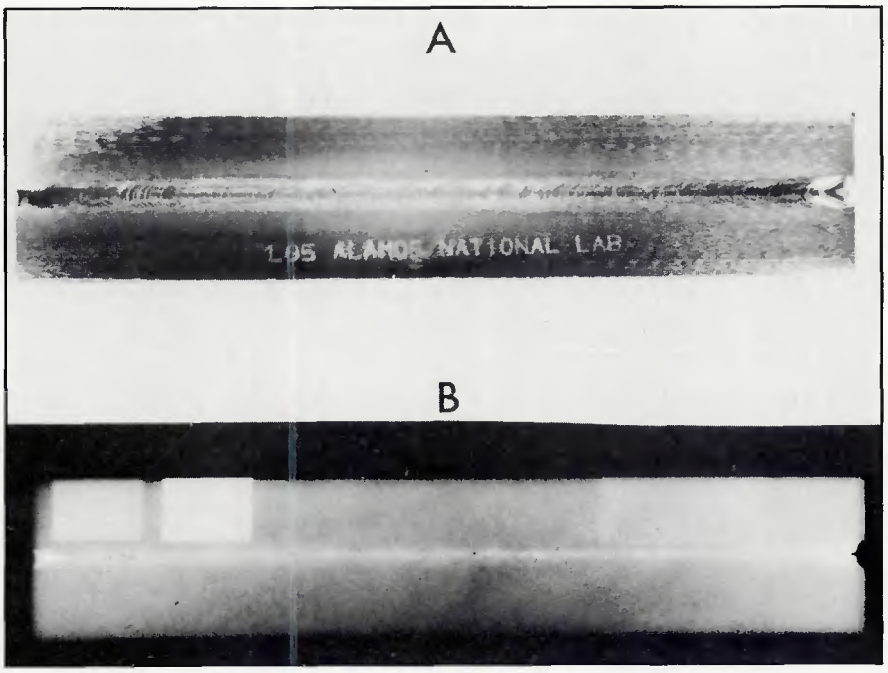

Fig. 3 — A — Photograph of a 127-mm (5-in.) long autogenous electron beam weld in XD TiAl. Note the uniform surface appearance and high quality. B — X-ray radiograph of the weld in A showing randomly dispersed porosity as the only detectable defect.

Results and Discussion

It was found that good quality fusion welds could be made on XD TiAl if correct process parameters were chosen. Figure 3A shows the weld produced at the lowest travel speed, 0.002 m/s, 300°C (572°F) preheat, HAZ CR = 35 K/s. The overall sound appearance of this weld is supported by the x-ray radiograph shown in Fig. 3B, in which randomly distributed spherical gas porosity was the only de-

Table 2—Welding Parameters[a]

Weld Speed (m/s)	Beam Voltage (kV)	Beam Current (ma)	Preheat (°C)	Cooling Rate[b] (°K/s)
0.002	150	2.2	27	90
0.006	150	2.5	27	650
0.012	150	4.0	27	1015
0.024	150	6.0	27	1800
0.002	150	2.2	300	35
0.006	150	2.5	335	200
0.006	150	2.5	170	400
0.012	150	4.0	335	310
0.006	100	2.0	470	325
0.012	150	3.5	27	1320

(a) 7.5 kW Hamilton standard electron beam system, 23 cm gun-to-work distance, sharp focus, vacuum = 10^{-5}.
(b) Calculated average heat-affected zone cooling rate (1400° to 800°C).

tectable defect. Since no effort was made to optimize cleaning procedures, the occurrence of porosity was anticipated.

Figure 4A shows a photomicrograph of a weld made using the lowest travel speed and no preheat, resulting in a calculated HAZ CR of approximately 100 K/s. Weld top and bottom contours are uniform and nearly flush with the base metal, indicating good molten pool fluidity and surface tension characteristics. The assumption of smooth molten metal flow was further supported by review of video monitor records of each weld that showed minimal pool disruption or turbulence. Furthermore, general observation of XD TiAl welds revealed characteristics similar to those of commercial titanium alloys and as such, considered to be quite good.

Metallographic specimens were evaluated by EDS to ensure that compositional changes were not occurring within the fusion zone. Within the resolution limits of this technique (approximately 2 wt-%), no variation in aluminum concentration between the base metal and fusion zone was observed.

Figure 4B, C and D show representative photomicrographs of the microstructural progression from the base metal to the fusion zone. Base metal microstructures have been discussed previously and are shown here for reference. In comparison, the HAZ microstructure (Fig. 4C) is slightly coarsened and has an increased amount of lamellar alpha-2-plus-gamma colonies. The fusion zone microstructure (Fig. 4D) consists of a relatively featureless matrix, a largely unaltered distribution of TiB_2 particles and a very small amount of a dark etching acicular microconstituent. This acicular microconstituent was not identified during the course of this investigation. However, in a study of atomized powder made from XD TiAl material, Kampe, *et al.* observed a similar microconstituent and identified it using x-ray diffraction as consisting of Ti and B (Ref. 10). These investigators assumed that the acicular microconstituent resulted from a morphological change of TiB_2 particles.

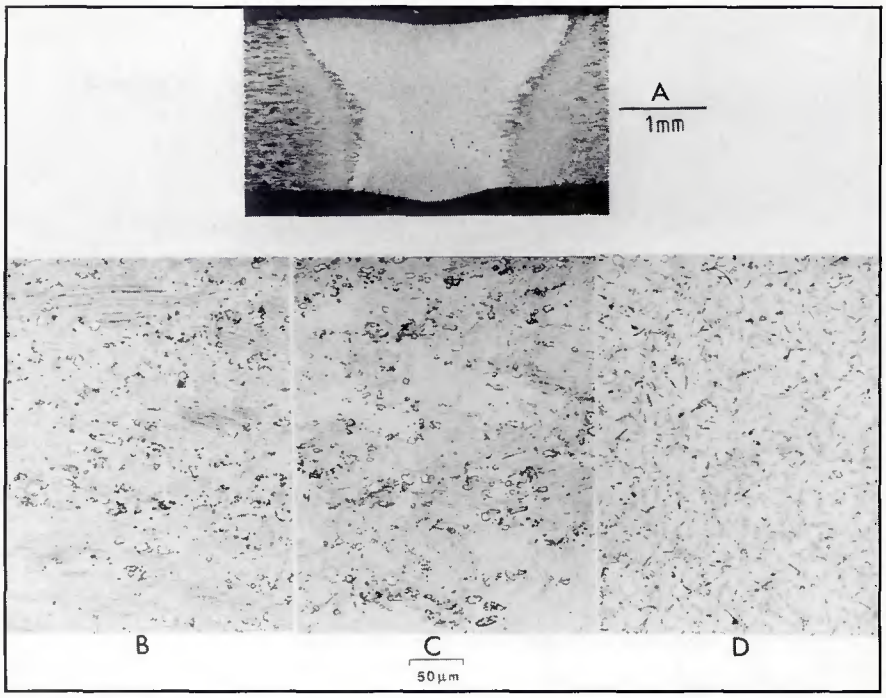

Fig. 4—Photomicrographs of 0.002 m/s weld cross-section. A—Uniform top and bottom weld contours indicate good molten metal fluidity; B—base metal; C—the heat-affected zone has a slightly greater amount of lamellar structure than does the base metal; D—the fusion zone consists of a featureless matrix, unchanged distribution of TiB_2 particles, and dark-etching acicular microconstituent. Modified Kroll's etch.

The principal difficulty encountered during the welding of this material was a susceptibility to weld cracking when the selected weld parameters resulted in high HAZ CR's. Figure 5 shows SEM photomacrographs of typical cracks as seen on the weld top surface. Cracking observed at high HAZ CR's (>400 K/s) can be described as large transverse cracks, that propagated into the base metal—Fig. 5A, and deviated to an angle of 45 deg to the welding direction before blunting and crack arrest. At intermediate HAZ CR's (300 to 400 K/s), cracking was seen to occur at the fusion boundary without extensive propagation into either base or weld metal—Figs. 5B and C. The widest crack opening associated with these small cracks was seen to coincide with the fusion boundary (Fig. 5C) suggesting that this location was the crack-initiation site.

Representative SEM fractographs of the fusion zone and base metal crack surfaces

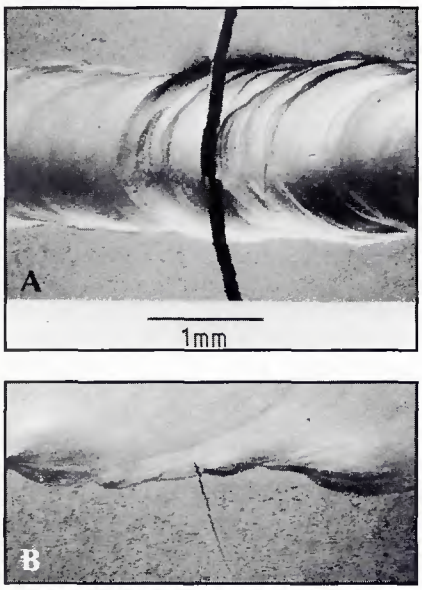

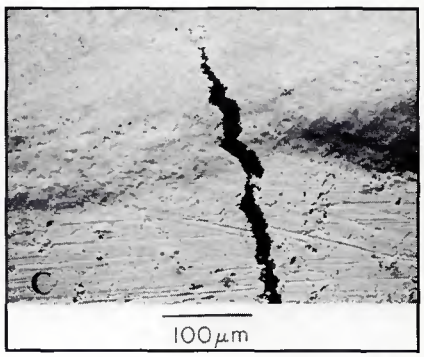

Fig. 5—Scanning electron micrographs of weld top surfaces showing the two types of cracks observed during this investigation. A—Large transverse cracking; B and C—smaller crack in which the maximum in crack width coincided with the fusion boundary.

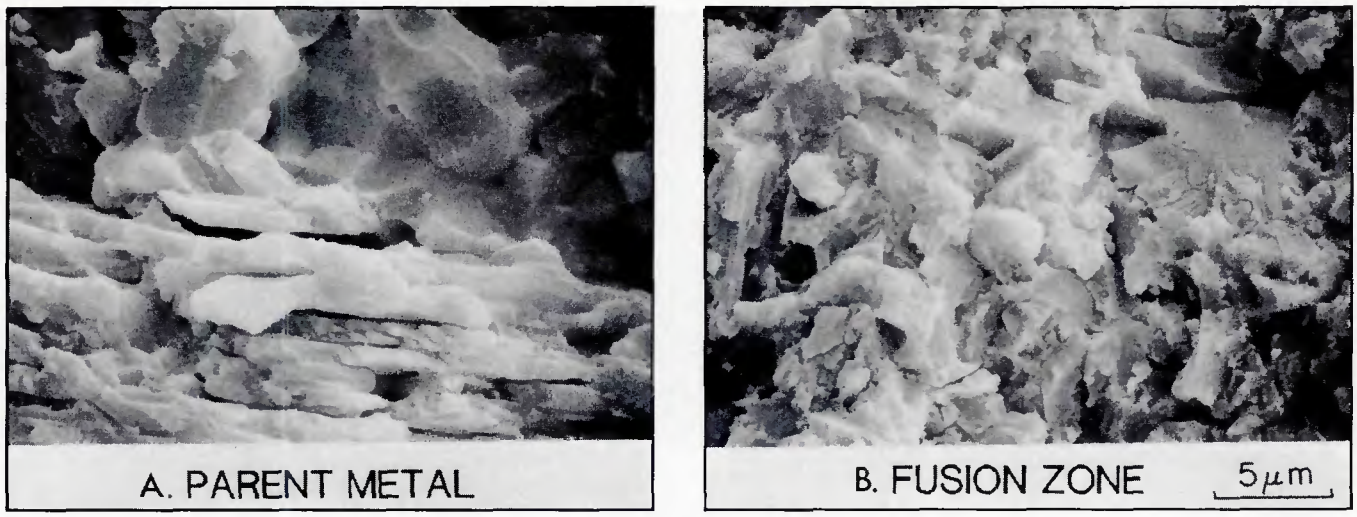

Fig. 6 — Scanning electron fractographs of crack surfaces observed. A — Base metal; B — fusion zone. Fracture occurred primarily by transgranular cleavage with some interlamellar separation.

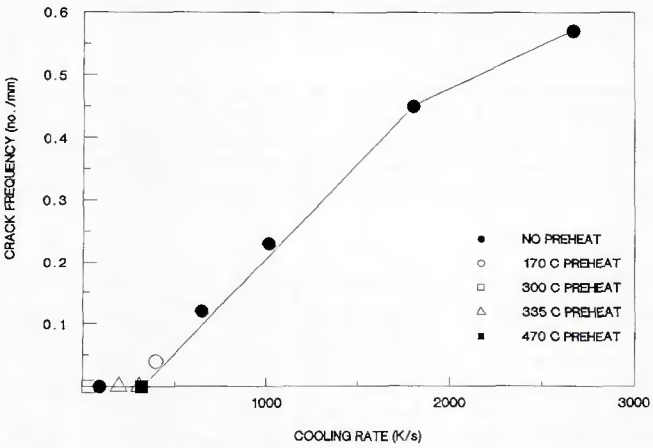

Fig. 7 — Cracking frequency versus calculated average heat-affected zone cooling rate (1400° to 800°C). Cracking initially occurs at a cooling rate of approximately 300 K/s and increases linearly with further increases in cooling rate.

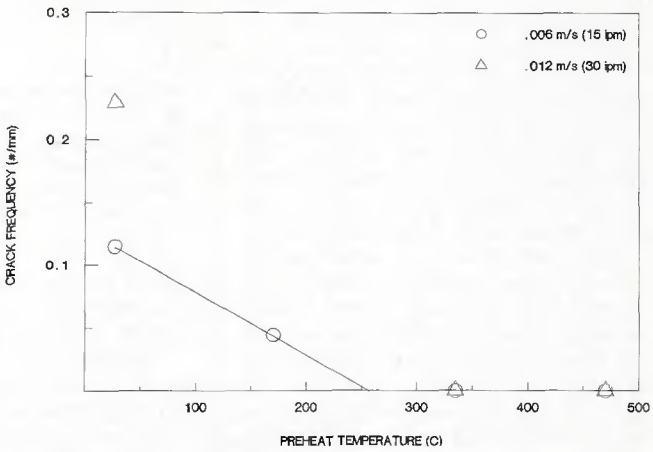

Fig. 8 — Crack frequency versus preheat temperature for welds performed at 0.006 and 0.012 m/s. Linear extrapolation of the 0.006 m/s data indicates that a minimum preheat temperature of 250°C is required to avoid weld cracking.

(Fig. 6) show that fracture occurred principally by transgranular cleavage. This figure also shows no evidence of grain boundary liquation or presence of fracture feature associated with the occurrence of subsolidus liquid microconstituents. Thus, traditional hot cracking was not the operative mechanism in this case. This was further substantiated by the video records, which show that cracking occurred in the solid state and at a significant distance from the molten pool.

In welds where cracking occurred, the spacing between cracks remained relatively constant along the length of an individual weld but varied between welds made using different parameters. This led to a characteristic cracking frequency for each weld, expressed as the number of cracks per millimeter of weld bead. Figure 7 shows the values of crack frequency plotted against calculated average HAZ CR. This figure illustrates two significant findings. First, in welds where cracking occurred, crack frequency varied linearly with cooling rate. Second, and most technologically significant, is the existence of a critical cooling rate below which cracking does not occur. Figure 7 shows this critical cooling rate to be in the range of 300 K/s. The occurrence of a cracking threshold can also be seen in Fig. 8, a plot of crack frequency versus preheat temperature for welds made at 0.006 and 0.012 m/s. A linear extrapolation of the data for welds made at 0.006 m/s indicates that a preheat temperature of at least 250°C (482°F) is required to avoid cracking. Calculated cooling rates for this set of welding conditions, 0.006 m/s weld speed and 250°C preheat, again suggests that the critical cooling rate is approximately 300 K/s. It must be noted that these cooling rates are calculated using thermophysical properties for a similar alloy, Ti_3Al-Nb, and as such can only be used to indicate trends. Thus, the existence of a critical cooling rate below which cracking does not occur is clearly shown, but the exact cooling rate cannot be calculated without thermophysical properties for the XD TiAl alloy.

Santella, *et al.*, reported a similar relationship between cooling rate and cracking susceptibility for electron beam welding of the Ni_3Al-based Alloy IC-25 (Ref. 12). Two similar alloys however, IC-50 and IC-103, were found to resist weld cracking at all weld speeds evaluated. It was concluded that the cracking of IC-25 occurred when thermally induced stresses exceeded the yield strength of the material in a temperature range where the material exhibited limited ductility. Decreasing weld speed or substituting an alloy with greater thermal conductivity (IC-50) reduced the thermally induced stress to below the material's yield strength. In contrast, Alloy IC-103 was found to be resistant to cracking even when the thermal stresses exceeded the yield strength because of the greater high-temperature

ductility possessed by this alloy.

Comparison with the results of Santella, *et al.*, suggests that the cracking observed in the XD TiAl material may result from a similar mechanism: specifically, thermally induced stresses exceeding the alloy's yield strength in a temperature range where ductility is minimal. To date, a detailed analysis of the thermal profiles and stresses developed during welding of XD TiAl has not been performed. However, it is reasonable to assume that the relationship between weld parameters and thermally induced stresses is similar to that seen in the IC-25 alloy. This assumption is supported by the microhardness measurements made on the XD TiAl weldments. Figure 9 shows the results of microhardness traverses across welds made at four different weld speeds. Welding at the slowest speed, 0.002 m/s, resulted in the smallest hardness increase between the fusion zone and the base metal, approximately 60%, and the largest affected area. As the weld speed was increased, the hardness increase became greater and was distributed over a smaller area. These results indicate that the thermal gradients become more severe as weld speed increases and imply that the thermally induced stress gradient increases as well.

An alternative explanation for the increase in cracking with increased cooling rate was suggested by an examination of the weld metal microstructures. Figure 10 shows the fusion zone microstructures for welds made at four different weld speeds (0.002 to 0.024 m/s). These photomicrographs show that the volume fraction of the acicular microconstituent discussed earlier increased significantly as the weld speed and cooling rate increased. The high aspect ratio of this microconstituent suggests that it may be acting as a stress concentration source and thus, a crack-initiation site. If this is the case, the increased cracking susceptibility of the high-travel-speed welds could be attributed to a reduction in ductility due to the presence of acicular microconstituent rather than to increases in the thermally induced stress. Low-speed welds then result in a situation analogous to the results of Santella, *et al.*, on the IC-103 alloy. Thermally induced stresses may exceed the material's yield strength, but there is sufficient ductility to absorb the necessary strain. To investigate the effects of microstructural changes, a more thorough characterization of fusion zone microstructures using x-ray analysis and transmission electron microscopy is currently in progress.

In summary, XD TiAl can be successfully welded using the electron beam technique when proper process parameters are selected. Parameters must be chosen to provide an average HAZ cooling rate below approximately 300 K/s. At higher cooling rates, the material is susceptible to cracking, which becomes increasingly severe with increasing cooling rate. These results, in combination with those of other investigators, suggest two possible mechanisms for the observed cracking and cooling rate dependence. First, high cooling rates induce thermal stresses that exceed the material's yield strength in a temperature range of limited ductility. Alternatively, increased cooling rates result in microstructural changes that reduce the material's ductility to below the level where thermally induced stresses can be accommodated.

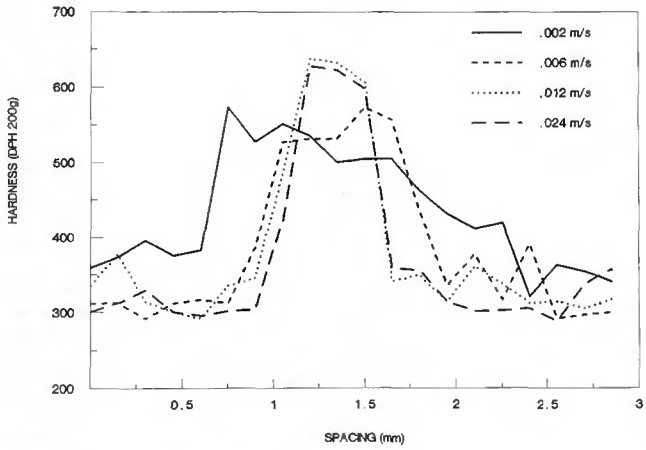

Fig. 9 — Microhardness profiles transverse to the weld direction for weld speeds ranging from 0.002 to 0.024 m/s. Slow speeds produced fusion zone hardness values approximately 60% greater than the base metal, while higher speeds resulted in significantly greater increases.

Conclusions

1) High quality electron beam welds can be made on the Alloy Ti-48 at.-% Al-6.5 vol-% TiB_2.

2) Susceptibility to solid-state cracking

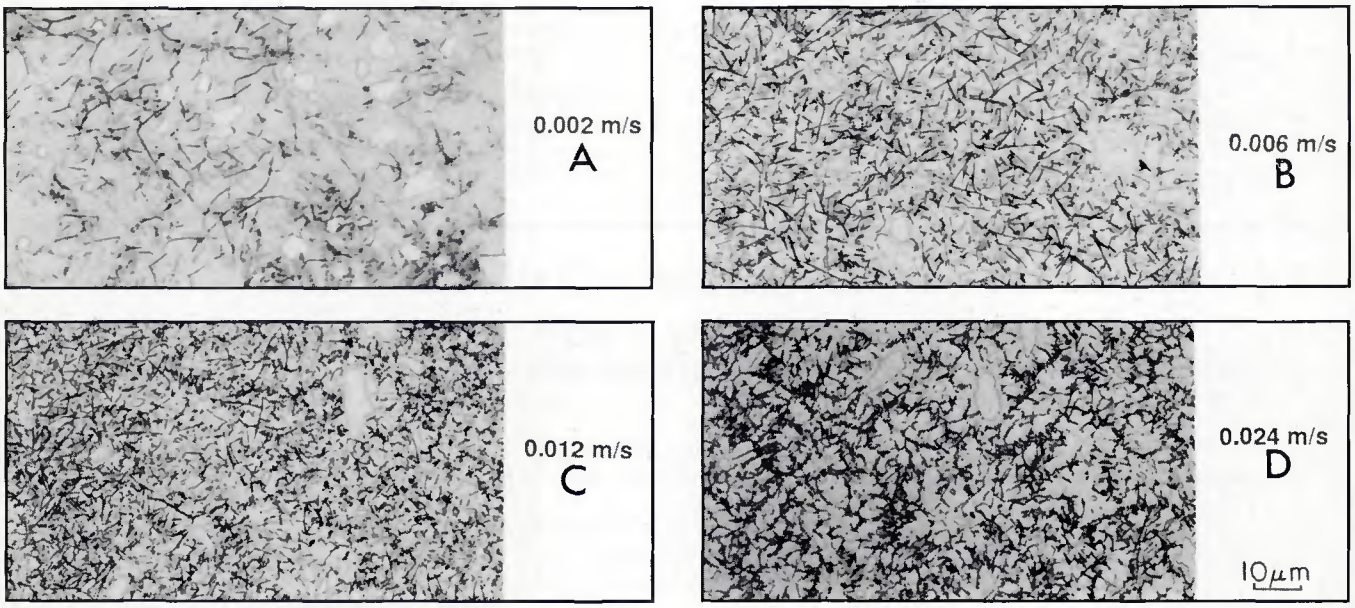

Fig. 10 — Fusion zone microstructures of welds made at speeds ranging from 0.002 to 0.024 m/s. Note the increasing amount of acicular microconstituent with increasing weld speed. Modified Kroll's etch.

was found to occur in some instances. Cracking initiated at the fusion boundary and proceeded by brittle transgranular cleavage.

3) Weld cracking can be avoided by the selection of welding parameters that result in calculated average HAZ cooling rates below approximately 300 K/s.

Acknowledgments

The authors wish to acknowledge the many coworkers and associates who have made contributions throughout the course of this investigation. Of particular note are Rob Aiken, Steve Kampe, and Melody Adams of Martin Marietta Laboratories, who supplied material and processing knowledge. At Los Alamos, Hugh Casey, Frank Smith, Ann Kelly, and Jim Bradbury deserve special note for their efforts. The authors also wish to acknowledge the support of the Department of Energy. Work was performed under the United States Department of Energy contract W7405-Eng36. Material supplied under NRL contract N00014-86-(227): R. C. Crowe, contract monitor; P. A. Parrish, technical leader.

References

1. Lipsitt, H. A. 1985. Titanium aluminides — an overview. *Proceedings of a Symposium on High-Temperature Ordered Intermetallic Alloys,* November 1984, Materials Research Society, vol. 39, pp. 351–364.

2. Stoloff, N. S. 1985. Ordered alloys for high-temperature applications. *Proceedings of a Symposium on High-Temperature Ordered Intermetallic Alloys,* November 1984, Materials Research Society, vol. 39, pp. 3–27.

3. *Structural Uses for Ductile Ordered Alloys,* 1984, National Materials Advisory Board, National Academy Press, NMAB-419.

4. Sprague, R. A. 1988. Future aerospace — materials directions. *Advanced Materials and Processes,* vol. 133, issue 1, pp. 67–69.

5. Santella, M. L., David, S. A., and White, C. L. 1984. Weldability of Ni_3Al-type aluminide alloys. *Proceedings of a Symposium on High-Temperature Ordered Intermetallic Alloys,* November 1984, Materials Research Society, vol. 39, pp. 495–503.

6. Santella, M. L., Horton, J. A., and David, S. A. 1988. Welding behavior and microstructure of a Ni_3Al alloy. *Welding Journal* 67(3):63-s to 69-s.

7. Mascorella, T. J. 1987. *Weldability of Ti_3Al-Nb Alloy,* MS Thesis, Ohio State University, Columbus, Ohio.

8. Christodoulou, L., Brupbacker, J. M., and Nagle, D. 1989. *Metallurgical Processes for the Year 2000 and Beyond.* Presentation given at TMS Annual Mtg., Las Vegas, Nev.

9. McCullough, C., Valencia, J. J., Levi, C. G., and Mehrabian, R. 1988. *The Processing and Mechanical Properties of High-Temperature High-Performance Composites,* University Research Initiative Annual Report, Book 6, Submitted to *Acta Metallurgica.*

10. Kampe, S. L., and Christodoulou, L. 1989. Microstructural evolution of rapidly solidified, ceramic-reinforced XD titanium aluminide composites. Submitted to *International Journal of Powder Metallurgy.*

11. Easterling, K. 1983. *Introduction to Physical Metallurgy of Welding.* Butterworths.

12. Santella, M. L., Maguire, M. C., and David, S. A. 1989. Analysis of heat-affected zone cracking in Ni_3Al alloy welds by computer modeling of thermal stresses. *Welding Journal* 68(1):19-s to 27-s.

WRC Bulletin 332
April 1988

This Bulletin contains two reports that characterize the mechanical properties of two different structural shapes of constructional steels used in the pressure vessel industry.

(1) Characteristics of Heavyweight Wide-Flange Structural Shapes
By J. M. Barsom and B. G. Reisdorf

This report presents information concerning the chemical, microstructural and mechanical (including fracture toughness) properties for heavyweight wide-flange structural shapes of A36, A572 Grade 50 and A588 Grade A steels.

(2) Data Survey on Mechanical Property Characterization of A588 Steel Plates and Weldments
By A. W. Pense

This survey report summarizes, for the most part, unpublished data on the strength toughness and weldability of A588 Grade A and Grade B steels as influenced by heat treatment and processing.

Publication of this Bulletin was sponsored by the Subcommittee on Thermal and Mechanical Effects on Materials of the Pressure Vessel Research Committee of the Welding Research Council. The price of WRC Bulletin 332 is $20.00 per copy, plus $5.00 for postage and handling. Orders should be sent with payment to the Welding Research Council, Suite 1301, 345 E. 47th St., New York, NY 10017.

WRC Bulletin 340
January 1989

Interpretive Report on the Mechanical Properties of Brazed Joints
By M. M. Schwartz

This report summarizes the mechanical properties, brazing procedures and testing of materials, such as aluminum, beryllium, copper, steel, nickel, superalloys, reactive metals, ceramics and graphite. Over 120 references are included in this interpretive report.

Publication of this report was sponsored by the Interpretive Reports Committee of the Welding Research Council. The price of WRC Bulletin 340 is $24.00 per copy, plus $5.00 for postage and handling. Orders should be sent with payment to the Welding Research Council, 345 E. 47th St., Suite 1301, New York, NY 10017.